Fuel 270 (2020) 117504

Contents lists available at ScienceDirect

Fuel

journal homepage: www.elsevier.com/locate/fuel

Full Length Article

Effect of interface elasticity on improved oil recovery in a carbonate rock from low salinity and ultra-low concentration demulsifier

Hyeyoung Cho, Taniya Kar, Abbas Firoozabadi*,[1]

Reservoir Engineering Research Institute, 595 Lytton Ave, Palto, CA 94301, USA

ARTICLE INFO

Keywords:
Enhanced oil recovery
Coreflooding
Demulsifier
Interfacial viscoelasticity
Wettability
Carbonate rock

ABSTRACT

The increase in oil recovery from low salinity water injection has been often attributed to the alteration of wettability to water wetting. The increase in elasticity of the interface may also contribute to increase in oil recovery as has been suggested in the literature.

In this work, we investigate oil recovery using two carbonate cores, one with large vugs, and the other without. The pore size and pore size distributions are very different in the two carbonate cores. The investigation centers on oil recovery from low and high salinity water injection, and by addition of an effective demulsifier molecule at 100 ppm in the injected high salinity water. The effective demulsifier molecule gives substantially higher oil recovery than low salinity and high salinity water injection. The oil-water interface elasticity increases significantly from the addition of 100 ppm demulsifier molecule to the aqueous phase. Salinity of the injected water is found to have a weak effect on oil recovery. We attribute high recovery performance of the 100 ppm surfactant to the increase in interface elasticity. The high recovery performance is observed in the carbonate reservoir rocks, both with and without vugs. The demulsifier molecule which is non-ionic has a very low adsorption in the carbonate rocks, around 2 mg/g at 100 ppm in high salinity injection water.

This work introduces a new process for improved oil recovery by the introduction of a demulsifier molecule at ultra-low cocentration. The molecule has limited effect on water-wetting. The critical micelle concentration (CMC) of the non-ionic surfactant in the injected brine is at 30 ppm. The low adsorption, and the CMC indicate that the molecule adsorbs at the oil-water interface. The conventional chemical flooding which may require one or two orders of magnitude more material is through significant reduction of interfacial tension. The interface elasticity is singled out to be the main contribution to improved oil recovery in this work.

1. Introduction

Waterflooding is the most widespread method in improved oil recovery [25,32]. Based on some of the earlier work on the effect of salt concentration on wettability, water imbibition, and oil recovery, in 1997, Tang and Morrow performed a systematic investigation of low salinity water flooding on improved oil recovery [39]. Before the work of Tang and Morrow [39] and more additionally since then, numerous hypotheses have been put forward to explain the increase in oil recovery by low salinity water injection [23,5,24,14,15,27,12,41,1,20,31]. Tang and Morrow [39] performed waterflooding experiments at different concentrations of salt in the injected water and in the connate water. In both cases a lower concentration of salt gave a higher oil recovery. All the tests were conducted at the same injection rate in sandstone cores. They reasoned the change to more water-wetting from low salt concentration to be the main process for improved oil recovery. Tang and Firoozabadi [38] have investigated the rate effect in oil recovery in water flooding at different wettability states. They found that at strong water-wetting, the injection rate does not affect the oil recovery at a given initial water saturation. In weak water-wetting condition, as the rate increases, the oil recovery can increase significantly. The experiments were performed in a chalk sample. The rates are within the capillary number considerations as discussed in Supplementary Information D.

In addition to wettability alteration which relates to the fluid-solid interactions, there are other effects that have been brought up including emulsion formation [30,22,36,44], clay migration [40], and multicomponent ions exchange. Change of interfacial tension from salt concentration is often small. An effect from ion exchange may be related to wettability [4]. Emadi and Sohrabi [9] investigated formation

* Corresponding author.
E-mail address: af@rerinst.org (A. Firoozabadi).
[1] Department of Chemical and Biomolecular Engineering, Rice University, Houston TX, 595 Lytton Ave, Suite B, Palto, CA 94301, USA.

https://doi.org/10.1016/j.fuel.2020.117504
Received 8 January 2020; Received in revised form 22 February 2020; Accepted 28 February 2020
Available online 13 March 2020
0016-2361/

of water micro dispersions at the interface of crude oil and low salinity water injection in a mixed wet system, through direct visualization in a series of micromodel experiments. They hypothesized the formation of water micro dispersions in the oil phase during low salinity water injection by release of surface active agents from the interface, altering wettability. These emulsions formed at the oil-low salinity water interface were found to coalesce, causing swelling of connate water droplets and remobilization of trapped residual oil.

Another potential mechanism in low salinity water injection that may affect oil recovery is from viscoelasticity of the fluid-fluid interface. Fluid-fluid interface viscoelasticity is a mechanical property while interfacial tension is a chemical property. It has been suggested that the oil-water interface viscoelasticity relates to the strength of oil-water films stabilized by asphaltenes and other polar fractions of crude oil [11,10,28,3,13]. Many studies show that the interfacial viscoelasticity may depend on the concentration and type of asphaltenes [3,13,37,29]. While interfacial tension may depend on the amount of asphaltenes at the interface, interfacial viscoelasticity is governed by the arrangement of molecules (molecular structure) at the interface. Asphaltenes are known to increase interface elasticity by gradual movement and alignment of molecules, thereby stabilizing water-oil emulsions. Higher asphaltene content in crude oil can lead to development of a slower, but more rigid network at the interface, leading to a high elasticity Freer et al. [11]. Spiecker and Kilpatrick [33] used an interfacial shear rheometer to study asphaltene stabilized films at oil-water interface by performing elasticity and yield stress measurements. Asphaltenes with varying aromaticity, heavy metal content, and polarity from different crude oils were separated and mixed in the heptol solution. Highly elastic, consolidated oil-water films resulted from the presence of asphaltenes having higher heavy metal concentration, polarity, and lower aromaticity. Additionally, higher concentration of aromatic solvent made the asphaltenes more solvated, resulting in films of lower elasticity, yield stress, and weaker emulsions.

In waterflooding, fluid-fluid viscoelasticity has been reported to affect oil recovery. Bidhendi et al. [6] reported the elastic modulus at the interface between sodium sulfate brine and a crude oil. The maximum elastic modulus was 38 mN/m at a brine concentration of 6.724 mM (Na_2SO_4 solution) and the elastic modulus decreased by increasing salt concentration. They used a microfluidic device to measure oil recovery at low brine concentration (6.724 mM of Na_2SO_4 solution) to be around 30% higher than in a high salinity brine (0.6724 M of Na_2SO_4 solution) injection. The authors suggest that the increase in oil recovery was because of the increased elasticity of the fluid-fluid interface, judged by an increase in elastic modulus. The increase in oil recovery was from reduction of the oil snap-off in the displacement.

Chávez-Miyauchi et al. [8] studied low salinity water injection in a water-wet sandstone; they found there exists a correlation between interface viscoelasticity and oil recovery. They observed improved oil recovery with low salinity water injection when there is an increase in fluid-fluid elasticity at low salinity. In some of the experiments by Chávez-Miyauchi et al. [8], without change in wettability from salt concentration change, an increased oil recovery was observed. The work by the authors was in in Berea sandstone cores in different oils. In one of the three whole crudes (K1), significant improved oil recovery was observed by low salinity water injection in comparison to high salinity water injection.

In the work above on viscoelasticity, interface elasticity is mainly described by elastic modulus. An increase in elastic modulus is generally referred to as an increase in interface strength and elasticity. The idea of interface elasticity increase from surfactants in injected brine was introduced by Chávez-Miyauchi et al. [7]. At 100 ppm surfactant concentration, the authors reported the interface elasticity increase resulted in 10% oil recovery increase. However, they used the phase angle as a measure of fluid-fluid interface elasticity. In interfacial viscoelasticity measurements, three parameters are measured: elastic (storage) modulus, viscous (loss) modulus, and phase angle. Phase angle is related to the ratio of viscous to elastic moduli; it ranges from 0 to 90° (°). The lower the phase angle is, the higher is the fluid-fluid interface. Chávez-Miyauchi, et al. found that the addition of the surfactant lowers both the elastic and viscous moduli compared to the case when no surfactant was added, but the overall phase angle was found to reduce. They attributed the increase in interface elasticity to the reduction in phase angle, accounting for both moduli. In this work, we compare the change in elastic and viscous moduli, as well as phase angle in relation to interface viscoelasticity. The original idea of the use of surfactant at 100 ppm concentration is from Sun et al. [36] where the authors observed a very large pressure drop and wild pressure fluctuations in water flooding of a relatively low viscosity oil. The surfactant at 100 ppm (demulsifier, DEM) was effective in preventing water-in-oil emulsion formation in the oil-water systems. Without the DEM in the injected water due to formation of water-in-oil emulsions a high pressure drop and large pressure fluctuations were observed in waterflooding. The addition of 100 ppm of demulsifier in injection water prevented formation of water-in-oil emulsions; and the pressure drop reduced significantly. Sun et al. [36] observed a final oil recovery increase of about 12% from 100 ppm demulsifier. In 2018, Kazempour et al. [19] examined improved oil recovery in shale rock from imbibition by a demulsifier at 1000 ppm. In their work, the improved recovery was attributed to significant wettability change from oil-wetting to water-wetting. They called the DEM as Production Enhancer (PE). The contact angle of the brine-crude oil-shale rock decreased from about 160° to 40° by the addition of the demulsifier at 1000 ppm demonstrating alteration of oil wetting to water wetting. Interfacial tension between the oil and high-salinity brine was reduced by an order at 1000 ppm concentration. The authors concluded the use of the demulsifier molecule alters wettability to water-wetting based on both wettability and water imbibition. Recently, Kar et al. [18] further studied the correlation between oil-water interfacial elasticity and oil recovery in a crude oil sample which gave high recovery from low salinity water injection and high salinity water injection at 100 ppm chemical. They performed waterflooding experiments in Edward Yellow carbonate cores saturated with a light crude oil. The addition of 100 ppm non-ionic surfactant to the injected brine increased the interfacial elasticity significantly (lowered phase angle). In the oil used by Kar et al. [18] the increase in interfacial elasticity by the chemical was independent of the salinity of the aqueous phase. The increases in recovery from low salinity and 100 ppm surfactant in high salinity were nearly the same.

In this work, we use the same non-ionic surfactant as in the past [36] and investigate the effect of the oil-brine interface elasticity on improved oil recovery in a crude oil for which the low salinity water injection has a weak effect on oil recovery. Two vastly different carbonate rocks (one with vugs, the other without vugs) are used. DEM at 100 ppm is dissolved in the injected water to examine the waterflooding performance. The oil and rocks are from the same field in the Middle East. We measure the contact angle and interfacial tension to examine the effectiveness of the demulsifier molecule at 100 ppm. We also measure the critical micelle concentration (CMC) in the brine. The concentration of the surfactant in the injected water should be above CMC [26,16]. The CMC primarily dependents on temperature and salinity of the aqueous phase. The effectiveness of the non-ionic surfactant in our work is due to low adsorption at the fluid-rock interface, and accumulation and structure at the oil-water interface. To investigate the selectivity of chemical to the interfaces in relation to efficiency of the demulsifier in waterflooding, adsorption of the surfactant on the rock surface is also measured. One objective of this work is investigation of increase in oil recovery by very low concentration of DEM in the injected high salinity water when low salinity water is not effective. We find the 100 ppm concentration of chemical is more effective than low salinity water injection. This is the first report of the process in relation to the comparison of interface elasticity with weak effect from low salt concentration and pronounced effect from 100 ppm

Table 1
Relevant properties of the crude oil at 25 °C.

ρ (g/ml)	μ (cP)	TAN (mg_{KOH}/g)	TBN (mg_{KOH}/g)
0.873 ± 0.0001	18.3 ± 0.1	0.268 ± 0.067	1.168 ± 0.049

demulsifier in two vastly different carbonate rocks, with and without vugs.

2. Materials and methods

2.1. Fluids

The relevant properties of the crude oil used in our investigation are listed in Table 1. Density, ρ, and viscosity, μ, of the oil sample are measured using an Anton Paar DMA5000 density meter, and an Anton Paar MCR 302 shear rheometer with 50 mm parallel plate geometry, respectively. Total acid number (TAN) and total base number (TBN) are obtained by performing potentiometric titrations using 1 g of oil [36]. Measurements are repeated from 3 to 5 times.

The crude forms strong water-in-oil emulsions when mixed with brine (see **Supplementary Information A**). The brine equilibrated with rock has much lower tendency to form emulsions in the oil. Details are presented in **Supplementary Information B**. Addition of the DEM further reduces the emulsion formation discussed also in **Supplementary Information B**.

Brines are prepared by mixing salts and DI water. Connate water is prepared based on the composition of the reservoir brine. High salinity and low salinity brines are from NaCl solutions. Compositions of the brines are presented in Table 2.

Toluene, dichloromethane, and methanol were purchased from Fisher Chemical; the purity is more than 99.5%. The three chemicals were used for cleaning the core samples after each waterflooding experiment. The demulsifier molecule in this work is a nonionic surfactant; the main functionality is the ethoxylated resin. It is an emulsion destabilizer. We used the same demulsifier (DEM) reported by Sun et al. [36].

2.2. Core samples

Two carbonate rock samples, Core #1; 1.5 in. in diameter and 2.4 in. in length and Core #2; 1.5 in. in diameter and 2.2 in. in length are used in waterflooding. Fig. 1 shows images of both cores; some of the pore (vug) sizes of Core #1 are large enough to be observed by naked eye. The pores of Core #2 are small and cannot be observed by naked eye. The mineral compositions of both cores are measured using X-ray diffraction analyses. Both cores have more than 99% calcite and less than 1% quartz. Micro-CT scanned images of Core #1 and Core #2 are shown in Fig. 2. Core #1 is scanned using Micro-CT at 40.16 μm resolution, 120 kV of voltage, and 2.5 s of the exposure time. Core #2 is scanned at 5.19 μm resolution since the pores are much smaller than Core #1. The 3D images of both cores are generated from the Micro-CT scanned images at different heights (see Fig. 3). As Fig. 3 reveals vugs exist inside Core #1, but not in Core #2.

Table 2
Brine composition.

	Salt Concentration (wt%)		
Salt	Connate Water	High Salinity (HS)	Low Salinity (LS)
NaCl	20.49	4.00	0.10
$CaCl_2$	5.60	—	—
$MgCl_2$	1.30	—	—
KCl	0.64	—	—
Na_2SO_4	0.05	—	—

From the Micro-CT scanned images, the pore size distribution can be obtained. Using the denoising and segmentation processes from the scanned images, the Micro-CT scanned images can be converted to the solid and pores [43,21]. Most of the pores are connected; the watershed segmentation is used to isolate each pore. The pore size distribution of the two cores are shown in Fig. 4. The figure indicates that the total frequency of the pores of Core #1 are much higher than Core #2, implying Core #1 has higher pore density than Core #2. The maximum frequency of Core #1 is at 140 μm, while Core #2 has the maximum frequency at 20 μm (see Fig. 4**(a) and (b)**). As Fig. 4 shows**,** most pores of Core #2 are less than 160 μm, however, Core #1 has many pores even larger than 700 μm.

Using the generated 3D images of both cores, the internal pore connectivity is shown in Fig. 5; Core #1 has more connected pores than Core #2. Figs. 3–5 also show internal vugs. Despite the large difference in pore sizes, the recovery from both cores are equally increased from fluid-fluid interface elasticity increases as we will show later.

We clean the cores after each test following the same procedure. First, 10 pore volume (PV) of toluene, then 10 PV of dichloromethane, and 10 PV of methanol are injected in this order from the bottom of the core in the vertical position. After flowing with fresh solvents, the core is placed in a Soxhlet device and several cycles of hot toluene followed by a mixture of dichloromethane and DI water are performed until the solvent around the core is clear. After the cleaning procedure, the core is dried in the oven at 80 °C overnight.

2.3. Experimental procedure

2.3.1. Interfacial viscoelasticity

Interfacial viscoelasticity measurements are performed using the Anton Paar MCR 302 rheometer, with the Dunoy ring. Controlled shear deformation oscillatory runs are performed in which strain amplitude and angular frequency of oscillations are kept constant at 1% and 0.5 rad/sec, respectively. The Dunoy ring is positioned exactly at the oil-aqueous phase interface, and oscillations are performed at every 15-minute interval. The applied torque leads to angular deflection of the measuring system, and the resulting shear stress is computed. Depending on the viscoelasticity, there might be a response lag due to the deformation; strain will lag stress. Sinusoidal responses of the resulting shear stress and strain are created, from which the lag between stress and strain is obtained. The lag is referred to as the phase angle, it is a measure of elasticity of the interface. The maximum phase angle is 90°. For elastic interfaces, phase angle is often lower, with a minimum of 0°. The three important parameters of interfacial viscoelasticity measurements are: phase angle, storage (elastic) modulus G' and viscous (loss) modulus G''. In the section on Results, variations of elastic and viscous moduli with change in aqueous phase salinity and surfactant addition, as well as the overall effect on phase angle will be discussed.

2.3.2. Interfacial tension

Kruss Processor Tensiometer K12 is used to conduct the interfacial tension (IFT) measurements by a Dunoy ring. Aqueous phases with varying salt concentration are used in our measurements: deionized water, low salinity water, high salinity water, and connate water. The effect of the non-ionic surfactant DEM at 100 ppm on IFT is measured. All measurements are carried out after allowing sufficient time for the molecules to stabilize at the interface; each measurement is repeated to obtain an accurate estimate. The measurements are conducted at room temperature.

2.3.3. Wettability

Contact angle measurements are performed using a goniometer setup to determine wettability of the rock substrate in the oil-brine system. The study of the effect of salt and DEM on the contact angle is

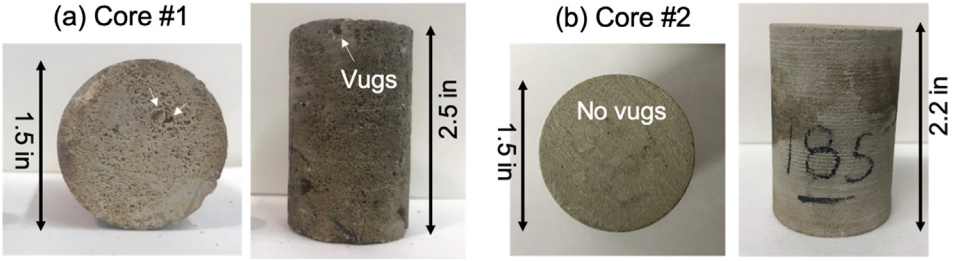

Fig. 1. Images of cores (a) #1 with vugs, and (b) #2 without vugs.

one of the objectives. First, the calcite substrate is aged with brine for a period of one day. Then, the oil droplet is placed on the substrate by a syringe. In some measurements we place up to 3 oil droplets on the substrate as shown in Fig. 6. The multiple droplets will provide standard deviations. After aging the oil droplet on the calcite substrate for three days, water-oil contact angle is measured using the Pendant drop method and the Drop Snake Plugin in Image software [34,35]. The procedure is discussed in detail by Aslan et al. [2]. We measure contact angle in different aging periods. It is found that the equilibrium is established in 3 days. The measured contact angle is based on the angle between the rock substrate and the outer edge of the oil droplet. An increase in the contact angle would imply more spreading of the oil on the rock, and an oil-wetting behavior. Similarly, a decrease in contact angle indicates a shift towards water-wetting behavior.

2.3.4. Core saturation

The core is saturated following the same procedure in all the tests. The core holder has a dead volume of 0.3 mL, about 0.15 mL in the inlet-side and about 0.15 mL at the outlet-side. A schematic of the waterflooding setup is depicted in Fig. 7. First, the core is vacuumed at 5 torr (0.097 psi, 0.0066 atm) for 40 min. Then, the core is saturated with DI water to measure the pore volume and porosity. The permeability is also measured by flowing DI water through the core at different flow rates. Then, the core is saturated with connate water by flowing 2 pore volume (PV) at 0.5 mL/min of flow rate. The system is closed and pressurized to 50 psi. Core is aged with connate water for 24 h.

After 24 h, the oil is injected until no water is produced. An extra PV of oil is injected and then the system is closed and pressurized to 50 psi. Core is aged with the oil for 72 h (3 days) before performing waterflooding. To examine the effect of longer aging time, in one waterflooding run, the core is aged with connate water for 3 days at 50 psi and then, aged with the oil for 3 weeks at 50 psi.

Relevant core properties are listed in Table 3. Note that after each coreflooding we measure porosity and permeability of the core.

2.3.5. Waterflooding procedure

In all the waterflooding experiments, the confining pressure is 200 psi. Water is injected at rate of 12 PV/d (0.1 mL/min) in Core #1 and at 4 PV/d (0.033 mL/min) in Core #2. Pressure is recorded at the inlet of the core. The outlet is open to atmospheric pressure. At the end of waterflooding, flow rate is increased five times to examine the end effect and wettability [38].

2.3.6. Cleaning procedure

Flooding with toluene, dichloromethane, and methanol are first performed to remove residual oil in the core. By performing Soxhlet cycles with solvents, the oil and chemicals are removed from the core completely. The permeability and porosity are the initial values after each cleaning procedure. The cleaning procedure is intended to keep the substrate in the same wetting state. In the past, using the procedure described above in duplicate corefloods has established reproducibility [8].

2.3.7. Adsorption measurements

Adsorption measurements are performed using the Perkin Elmer Lambda XLS UV–vis Spectrometer. The carbonate rock is crushed into particles of average size 210 μm. High salinity brine is equilibrated with the crushed rock for a period of 24 h. Then, various concentrations of demulsifier in equilibrated high salinity brine, ranging from 20 to 100 ppm, are prepared, and absorbance spectra are measured in the spectrometer. A wavelength of 230 nm is selected to compare the absorbance at different concentrations, and a concentration calibration plot for the demulsifier in high salinity brine is prepared. Next, solutions of demulsifier in high salinity brine are mixed with crushed rock (10 mL of brine mixed with 0.1 g of rock). These are allowed to stand in vials for a period of 24 h. Then the absorbance of supernatant is again measured and the concentration of demulsifier in the supernatant is

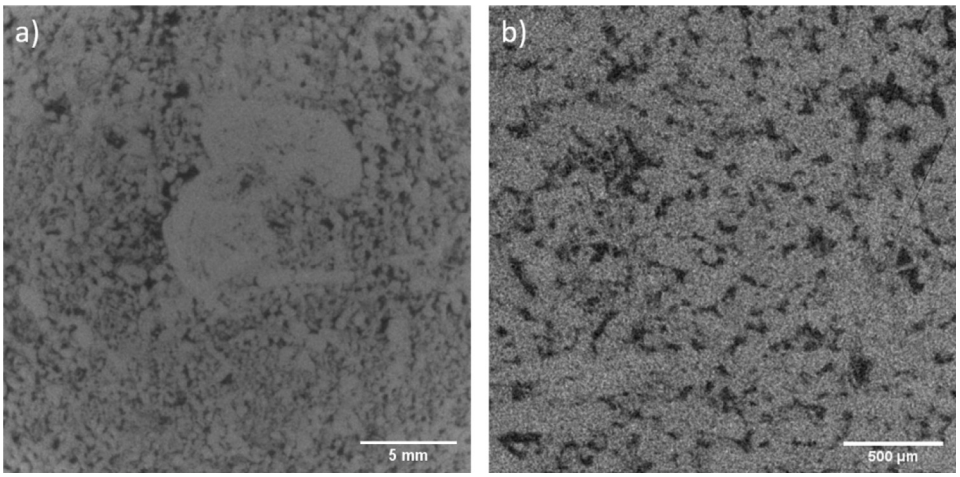

Fig. 2. Micro-CT scanned images of Cores (a) #1, and (b) #2. The scales of (a) is much higher than (b).

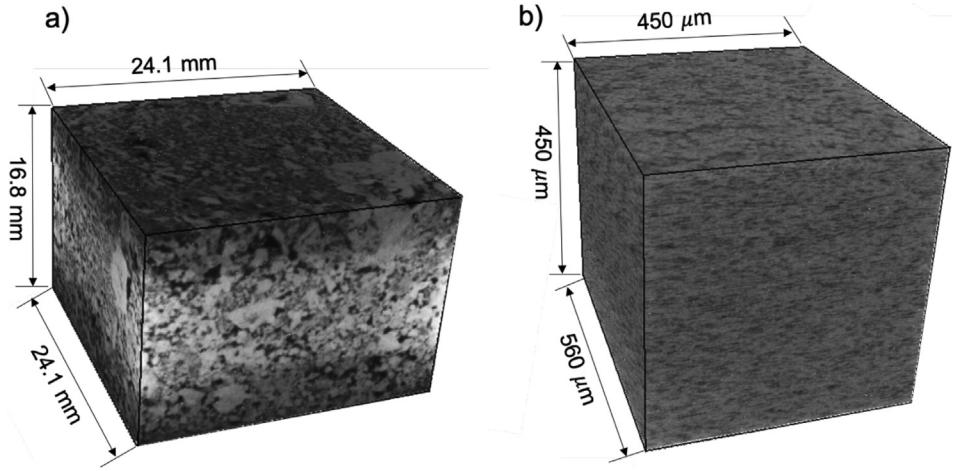

Fig. 3. 3D images generated from Micro-CT scanned images of Cores (a) #1, and (b) #2.

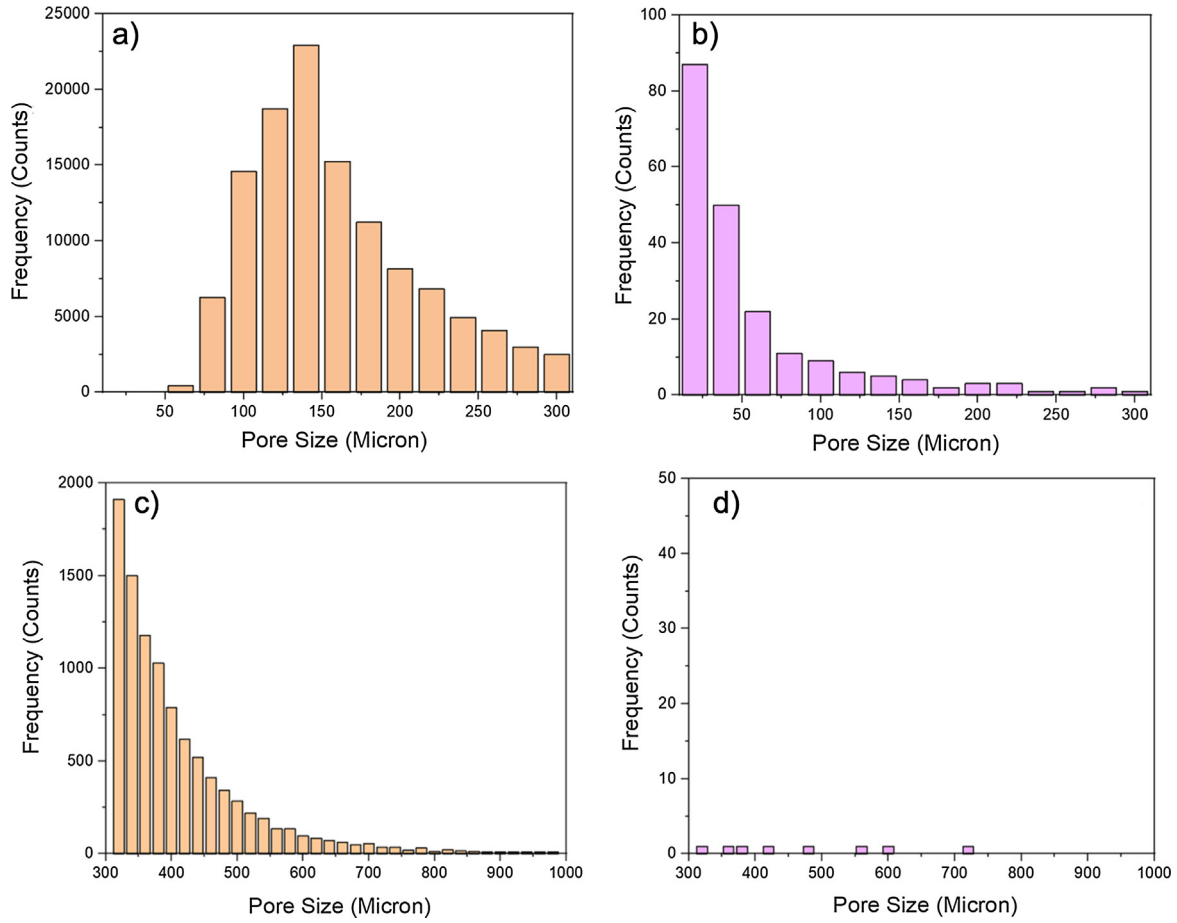

Fig. 4. Pore size distribution to 300 μm: (a) Core #1, and (b) Core #2, and in the range of 300 to 1000 μm: (c) Core #1, and (d) Core #2.

determined using the calibration plot. The adsorbed amount of demulsifier in the rock is then determined.

2.3.8. CMC measurement

Surface tension is measured at various concentrations of surfactant DEM in high salinity brine, and the results are plotted to obtain CMC. Above CMC, the surface tension (ST) tends to stay nearly constant. When plotted against a logarithmic concentration scale, two straight lines may be observed, one in the decreasing ST region, the other in the region where the ST is nearly constant. Intersection of these two straight lines provides the surfactant CMC at given temperature and salinity conditions.

3. Results and discussion

3.1. Interfacial viscoelasticity

The plots on development of storage modulus (G') and loss modulus (G'') with time for all the runs are presented in **Supplementary Information C (Figures C-1 to C-5)**. The final stabilized values of G' and G'' from these figures, along with the phase angle (δ) are listed in Table 4. In various aqueous phases, except the connate brine, the

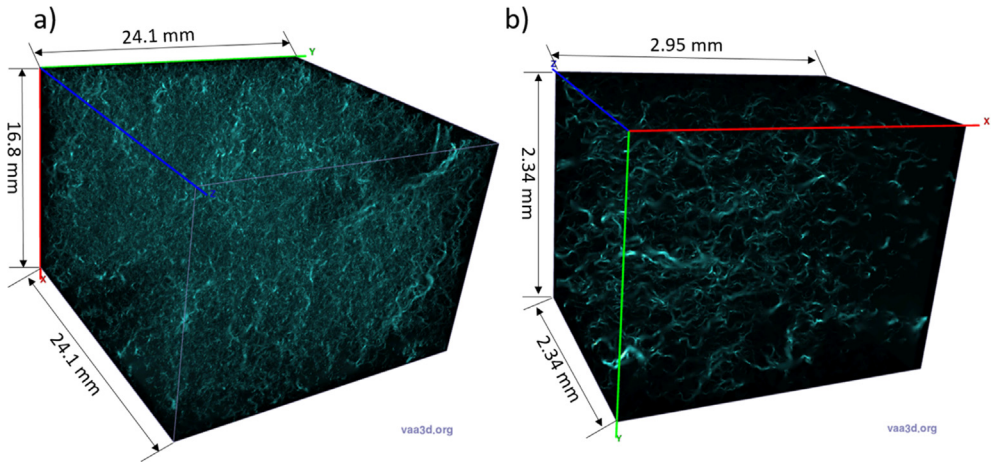

Fig. 5. 3D images showing the internal pore connectivity of Cores (a) #1, and (b) #2.

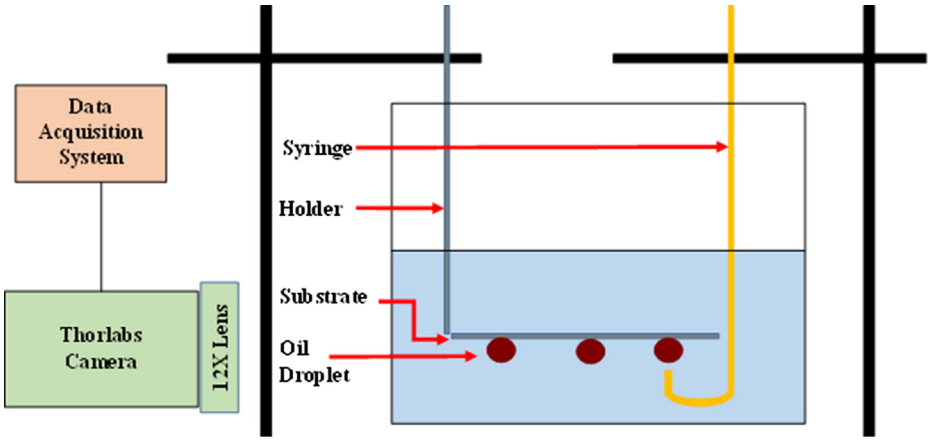

Fig. 6. Schematic of goniometer setup for contact angle measurements.

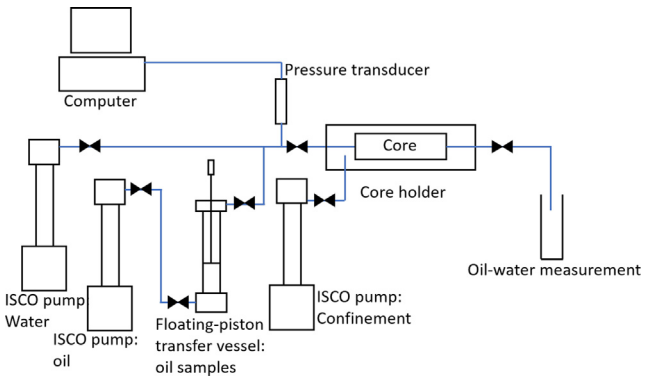

Fig. 7. Experimental setup for waterflooding experiments.

addition of demulsifier lowers both the elastic and viscous moduli considerably. The addition of demulsifier to the high salinity wáter destabilizes the wáter-oil emulsions, and breaks the emulsions as observed in vial tests (**Fig. A-1**) and from microscopic images (**Fig. A-2**). This is related to the lowering of G' by demulsifier. Similar observations were reported by Varadaraj and Brons [42] and Kang et al. [17]. However, as we will discuss later, in this work, the combined contribution of the elastic and viscous moduli, through phase angle, correlates with oil recovery in different coreflood experiments.

The effect on G' and G'' without and with demulsifier may depend on salinity as well as salt composition. In NaCl salt, surfactant reduces both G' and G'', and results in lowering of the phase angle. In the divalent ions (connate brine), surfactant increases G' and lowers G'', and reduces the phase angle. In this study, we have used phase angle as a measure of interface elasticity of the oil-water interface in different aqueous phases.

For a better understanding of the phase angle, we present the sinusoidal response of the shear stress with respect to the strain for a given time interval in **Fig. C-6**. The lag between the peak shear stress (σ_o) and peak strain (γ_o) at each interval is the phase angle (δ). For a completely elastic interface, there will be no lag; the phase angle is 0. As the interface elasticity decreases, the lag increases, increasing the phase angle. As seen from Table 4, a small concentration of demulsifier affects the moduli which results in lowering of the phase angle which make the oil-water interface more elastic. Additionally, changing concentration of DEM from 100 to 200 ppm in high salinity water does not significantly alter the viscoelasticity. This will be supported by coreflooding results using 100 and 200 ppm DEM in high salinity brine to be discussed later. We have repeated three interface viscoelasticty measurements in Table 4. For these three measurements the standard deviations are computed.

Fig. 8 depicts the plot of the phase angle data from Table 4. The figure illustrates significant effect of the DEM at 100 ppm on the increase in elasticity of the interface. The DEM lowers G', it also lowers G''. The change in rheology is due to accumulation of the surfactants at the oil-water interface and significant reduction of the phase angle. The same trend has been observed by Chávez-Miyauchi et al. [7].

Table 3
Water injection tests and relevant core properties.

Test	Core	Injection Water	Injection rate (PV/d)	PV (ml)	ϕ (%)	K_W (mD)	OOIP (ml)	S_{WI} (%)
1	#1	LS	12	11.5	17.6	452	8.9	22.7
2	#1	HS-DEM 100 ppm	12	11.1	17.0	423	8.2	26.1
3	#1	HS	12	11.8	18.0	421	8.8	25.4
4	#1	HS-DEM 100 ppm	4	11.9	17.1	458	8.8	21.4
5	#1	HS	4	11.7	17.9	433	9.3	20.2
6	#1	HS-DEM 200 ppm	4	11.3	17.3	423	9.3	17.7
7	#2	HS-DEM 100 ppm	4	13.9	22.7	41	10.2	26.3
8	#2	LS	4	14.7	24.1	41	9.8	33.9
9	#2	HS	4	15.0	24.5	37	10.3	31.6
10*	#2	HS	4	15.6	25.5	56	10.4	37.4

*longer aging time (3 days for brine, 3 weeks for the crude oil).

3.2. Interfacial tension

Table 5 presents the IFT data of the oil and aqueous phase: deionized water, low salinity water (0.1 wt% NaCl), high salinity water (4 wt% NaCl), and connate water (28 wt% salinity). IFT measurements are compared without and with 100 ppm of non-ionic surfactant DEM in the aqueous phase. The surfactant lowers the IFT at 100 ppm. However, the lowered values of IFT from DEM (lowest value = 0.78 mN/m) are not believed to be sufficient enough to effect a change in residual oil saturation. The data are plotted in Fig. 9.

3.3. Wettability: effect from salt concentration on Oil-Water contact angle

The contact angle measurements are divided into two parts. First, we present the effect of salt concentration on the wettability of the calcite substrate. Then, we examine the effect of surfactant at 100 ppm in the aqueous phase.

Fig. 10 reveals a general shift towards oil-wetting behavior as the aqueous phase changes from deionized water to connate water (reservoir brine) which has a salinity of 28 wt%. This trend is similar to the work by Aslan et al. [2].

3.4. Wettability: effect of demulsifier on oil-water contact angle

Next, we measure the effect of the non-ionic surfactant DEM on contact angle at 100 ppm dissolved in the aqueous phase. The surfactant results a shift towards water-wetting, as illustrated in Fig. 11. The size of droplets in Figs. 10 and 11 are not the same. When 100 ppm of DEM is added to the aqueous phase, it reduces the interfacial tension as presented above. As we place the oil droplet onto the substrate, part of the droplet may break off and the main droplet may become smaller when compared to the one without DEM. In both cases with and without DEM, we allow enough time for the system to reach the equilibrium (3 days). The interface flatness in the middle in Fig. 11 is from the low IFT effect.

The variation in contact angle with salt concentration without and

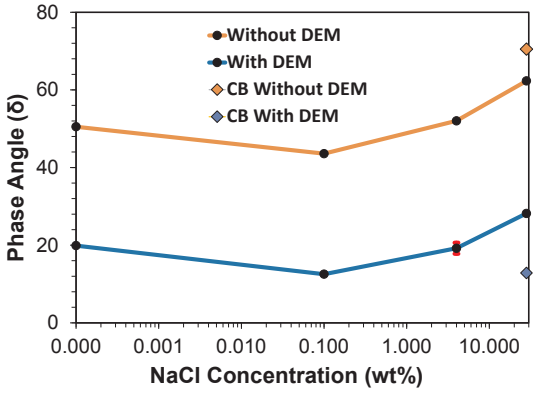

Fig. 8. Phase angle vs. NaCl salt concentration in the aqueous phase, without surfactant DEM (orange) and with 100 ppm surfactant DEM in aqueous phase (blue); comparison with reservoir brine without DEM (orange diamond) and reservoir brine with 100 ppm DEM (blue diamond) *CB- Connate (Reservoir) brine. (For interpretation of the references to colour in this figure legend, the reader is referred to the web version of this article.)

Table 5
Oil-aqueous phase interfacial tension measurements with aqueous phases of different salt concentrations, Without DEM and with 100 ppm DEM in the aqueous phase.

Brine Type	Salt Content (Wt%)	IFT (mN/m) of oil – brine	
		Without DEM	With 100 ppm DEM
Deionized water	0.00	19.6 ± 0.26	0.78 ± 0.15
Low salinity water	0.10	17.6 ± 0.15	0.90 ± 0.01
High salinity water	4.00	16.8 ± 0.16	0.89 ± 0.01
Connate water	28.08	15.4 ± 0.05	1.88 ± 0.13

Table 4
Relevant data from interfacial viscoelasticity measurements of the oil/aqueous phase. Salt is NaCl. The symbol * indicates duplicate tests.

Brine Type	Salinity (wt%)	DEM Concentration in Injected Water (ppm)	Storage Modulus G' (mN/m)	Loss Modulus G'' (mN/m)	Phase Angle δ (deg)
Connate water	28.08	–	0.1	0.4	70.5
		100	0.4	0.1	12.9
Connate brine NaCl	28.08	–	1.2	2.3	62.3
		100	0.1	0.05	28.2
High salinity	4	–	5.4	6.9	52.0
		100	0.2 ± 0.04*	0.06 ± 0.01*	19.2 ± 1.4*
		200	0.1	0.03	18.3
Low salinity	0.1	–	10.3	9.8	43.6
		100	0.2 ± 0.01*	0.05 ± 0.01*	12.5 ± 0.05*
Deionized water	0	–	4.4	5.4	50.5
		100	0.2 ± 0.01*	0.1	19.9 ± 0.1*

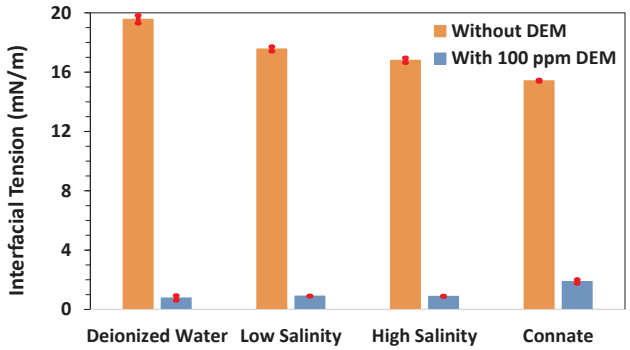

Fig. 9. Oil-aqueous phase interfacial tension: aqueous phases of different salt concentrations; without DEM and with 100 ppm DEM in the aqueous phase.

with surfactant is presented in Fig. 12. A non-monotonic trend is observed; decrease of contact angle, implies more water-wetting from the 100 ppm DEM. The trend, of contact angle vs. salt concentration is similar with and without DEM. As a whole the increase in water-wetting from the DEM is not pronounced.

3.5. Waterflooding performance: core with vugs

The essence of the waterflooding performance for different injection waters in Core #1 is shown in Fig. 13. Three types of brines include: low salinity water (LS, 0.1 wt%), high salinity water (HS, 4 wt%), and high salinity water with 100 ppm of DEM (HS-DEM). The water is injected from one side of the saturated core at 12 PV/d (0.1 mL/min) and after around 3 PV, we increase the flow rate to 60 PV/d (0.5 mL/min) to examine the end effect and wettability behavior of the core.

As shown in Fig. 13, the breakthrough time and recovery of LS and HS are close to each other (22%, 23%, respectively), however, HS-DEM has a later breakthrough (31%). The oil recovery increases steeply to breakthrough, and after breakthrough the slope decreases until recovery plot becomes flat. The oil recovery of the HS-DEM is higher than from HS and LS injection. There is extra oil recovery by increasing the flow rate from 12 PV/d to 60 PV/d for the three injections. The extra recovery can be from the end effect or from wetting being different from strong water wetting [38]. The HS-DEM shows the weakest effect from rate increase. The LS run shows the highest effect from the rate increase. The IFT reduction from 100 ppm DEM reduces the end effect. In the LS because of stronger water-wetting than the HS, the end effect may be more pronounced. The extra recovery from the rate increase does not change the overall trend. The oil recovery (54%) of HS-DEM at higher flow rate is higher than the other oil recoveries (HS: 48%, LS: 51%). This result shows the effectiveness of a small amount of demulsifier molecule on oil recovery. The improved recovery from addition of small amount of demulsifier may be related to the phase angle from interfacial viscoelasticity measurements (Fig. 8). Phase angles for high salinity (52°), low salinity (43.6°), and high salinity with surfactant (19.2°) correlate with the oil recovery, with the highest recovery from high salinity with the surfactant. The oil-brine IFT (Fig. 9) and the oil recovery data, reveal that the increased recovery in low salinity water injection compared to high salinity is not from IFT effect. Interface elasticity, and not the interfacial tension can be a key parameter governing the oil recovery performance.

In Fig. 14, the pressure drop profiles are shown. The pressure drops in LS and HS are close to each other, which is about 1.7 psi. Once the flow rate is increased to 60 PV/d, the pressure drop increases to about 2.6 psi in both the LS and HS waterflooding. The pressure drop of the waterflooding with HS-DEM 100 ppm is lower (0.7 psi) than the two others. Also, the extent of the increase of pressure drop by increasing the flow rate is lower than the other two. The pressure drop of HS-DEM at 100 ppm increases to 1 psi from rate increase. The pressure drop is not proportional to rate increase most likely due to small number of emulsions in the fluid system.

Emulsion formation and the effect of DEM on emulsion stability are also studied (see **Supplementary Information A**). The mixture of the oil and HS forms emulsions and DEM destabilizes emulsions significantly which supports that the pressure drop profile of waterflooding with DEM (HS-DEM) to be lower than LS and HS water injection. The emulsion formation in water equilibrated in crushed rock is also investigated (see **Supplementary Information B**). The emulsion tests without the rock require longer time for the oil-water mixture to separate.

The salinity and pH profiles of produced water in different water injections are shown in Fig. 15. Salt concentration drops with injected PV to 4 wt% for HS and HS-DEM at 100 ppm and to 0.1 wt% for LS waterflooding. pH stays the same during the waterflooding for all three tests implying that there is no significant dissolution of the minerals from the core. The pH of the injected waters is shown at PV of zero; it is somewhat lower than the pH of the produced water. The pH of the brine equilibrated in crushed rocks are measured as well (see **Supplementary Information B**).

We have also measured the pH and salt content of the produced water for the core without vugs to be described next. The trends are very similar to those in Fig. 15. The results are presented in **Supplementary Information D**.

3.6. Effect of the concentration of DEM on waterflooding performance

The effect of concentration of DEM on waterflooding performance is studied at two different concentrations of DEM (100 ppm and 200 ppm). As shown in Fig. 16, there is no significant effect of the concentration of DEM on the oil recovery. The breakthrough recoveries (35% and 36% for HS-DEM at 100 ppm and 200 ppm, respectively) are close and oil recovery in both is 57%. As mentioned before, there is no appreciable effect of DEM concentration of 100 and 200 ppm on interface viscoelasticity (Table 4).

3.7. Waterflooding performance: core without vugs

The waterflooding performance in Core #2, which has no vugs, is shown in Fig. 17; the oil recovery trend is the same as in Core #1. The oil recovery at high salinity at 100 ppm DEM is the highest among three different corefloods, higher than the low salinity (LS) and high salinity (HS) water injections. As shown in Fig. 17, the breakthrough time and recovery of LS and HS are close to each other (36%, 35%, respectively); HS-DEM has a later breakthrough (44%). The breakthrough time in Core #2 is later than in Core #1. The oil recovery increases steeply tol breakthrough, and after breakthrough the increase is not significant

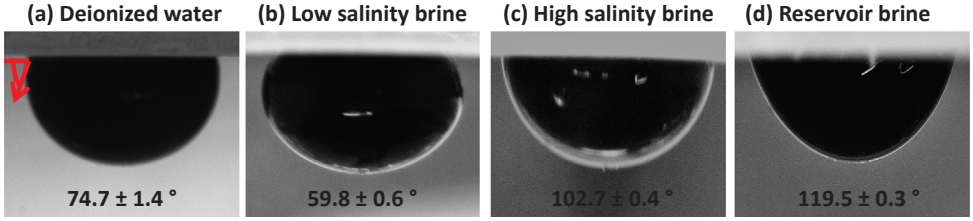

Fig. 10. Contact angle of the crude oil-water-calcite substrate in different brines: (a) Deionized water (b) Low salinity water (c) High salinity wáter, and (d) Reservoir (connate) brine.

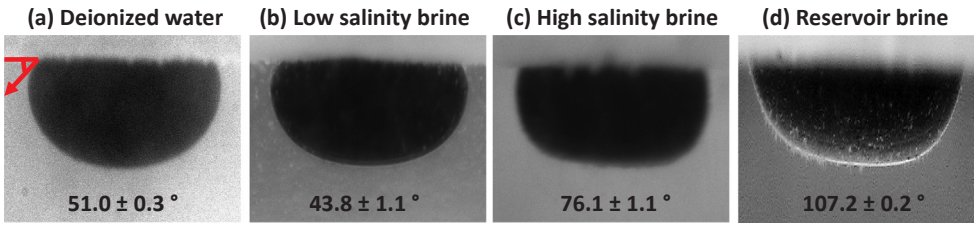

Fig. 11. Contact angle of the crude oil-water-calcite substrate with 100 DEM: (a) Deionized water, (b) Low salinity water, (c) High salinity water, and (d) Reservoir (connate) brine.

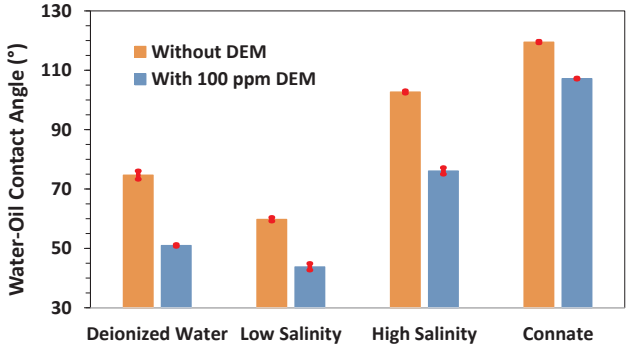

Fig. 12. Oil-aqueous pase-calcite contact angle measurements; aqueous phases of different salt concentrations; without DEM and with 100 ppm DEM in the aqueous phase.

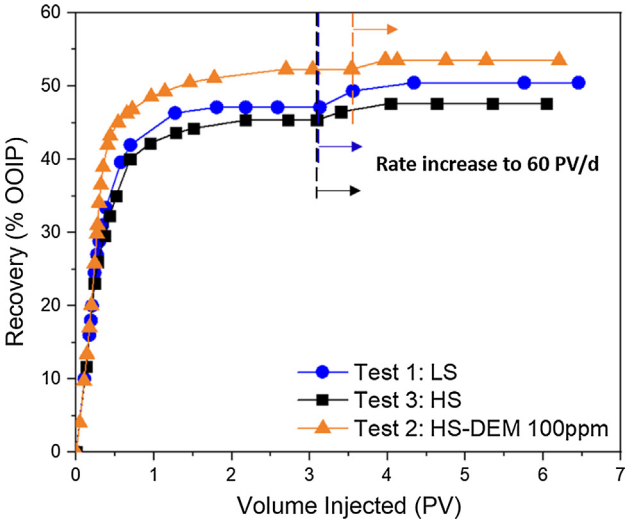

Fig. 13. Oil recovery performance by LS, HS, and HS-DEM at 12 PV/d of injection rate: Core #1.

until recovery becomes flat. There is extra oil recovery by increasing the flow rate from 4 PV/d to 20 PV/d implying the end effect or a wettability other than strongly water wetting [38]. The oil recovery at higher rate in HS-DEM (58%) is higher than the other oil recoveries (HS: 53%, LS: 54%). The results show the effectiveness of a small amount of demulsifier molecule on oil recovery.

The emulsions in the produced oil is examined after each waterflooding. In the three corefloods with LS, HS, and HS-DEM, we do not observe emulsion in the produced oil under the microscope. There is also no emulsion in the produced water. The effect of rate increase is very similar in Figs. 13 and 17.

In Fig. 18, the pressure drop profiles during the waterflooding are shown. The pressure drops of LS and HS are close to each other, which is about 15 psi before increasing the flow rate. Once the flow rate is increased to 20 PV/d, the pressure drop increases to about 45 psi for LS and 28 psi for HS waterflooding. However, the pressure drop of the waterflooding performance of the HS-DEM at 100 ppm is lower (3.2 psi)

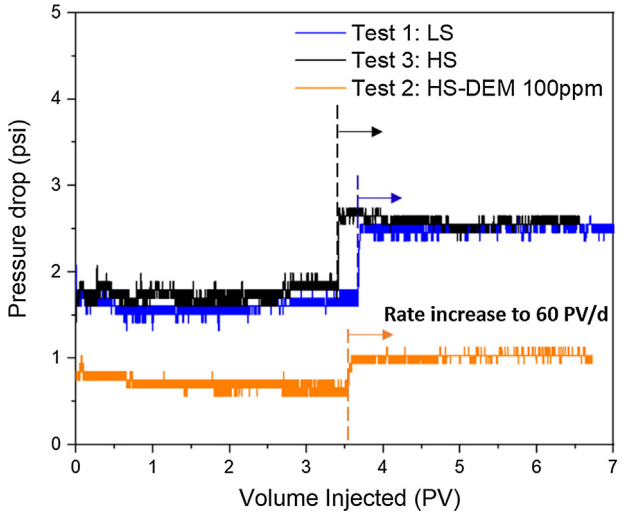

Fig. 14. Pressure drop profile of waterflooding with LS, HS, and HS-DEM at 12 PV/d of injection rate: Core #1.

than the two others. Also, the extent of the increase of pressure drop by increasing the flow rate is lower than the two others. The pressure drop of HS-DEM at 100 ppm increases to about 16 psi from flow rate increase.

3.8. Effect of longer aging time on waterflooding performance

We have examined the effect of longer aging time in both brine saturation and oil saturation on waterflooding performance in Core #2. We aged the core for 3 days in brine and 3 weeks in oil. Except this run, 1 day for brine and 3 days for oil is used as an aging condition. As shown in Fig. 19, there is no significant effect of longer aging time on oil recovery; the final oil recovery from long aging time (52%, test 10) is close to shorter aging time (53%, test 9).

3.9. Adsorption measurements

The absorbance spectra (ranging from 220 to 300 nm wavelengths) for demulsifier in high salinity brine are shown in Fig. 20**(a)**. There is a consistent increase in absorbance with increase in demulsifier concentration in brine. Due to adsorption in the rock, there is a slight decrease in absorbance at different concentrations. The calibration plots based on the absorbance in Fig. 20**(a)** are presented in Fig. 20**(b)**.

Table 6 reveals that adsorption of demulsifier in the carbonate rock ranges from 0.4 to 2 mg/g. The equivalent adsorption in terms of surface area of rock is quite small. There is lower adsorption at the rock surface as the salt concentration decreases. For a more realistic determination of adsorption of the chemical in the core during waterflooding, we have performed dynamic adsorption [18], in which we aged a carbonate rock with high salinity brine, then injected high salinity brine mixed with the 100 ppm of the non-ionic DEM and measured the concentration of chemical in the produced water via the same technique described in this study. Concentration of surfactant in the produced water dipped to 80 ppm after 2 PV injection, and

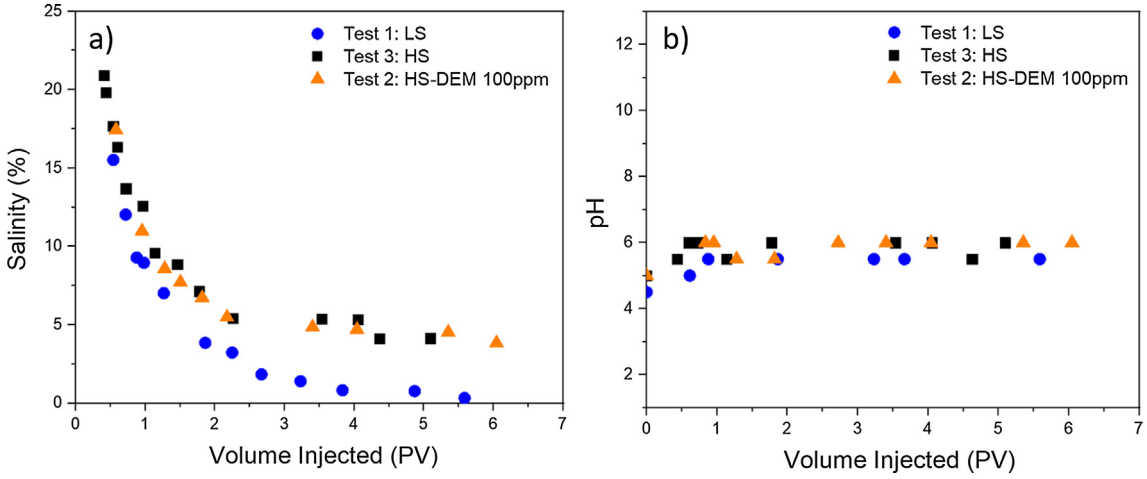

Fig. 15. a) Salt concentration, and b) pH profile of produced water of LS, HS, and HS-DEM: Core #1.

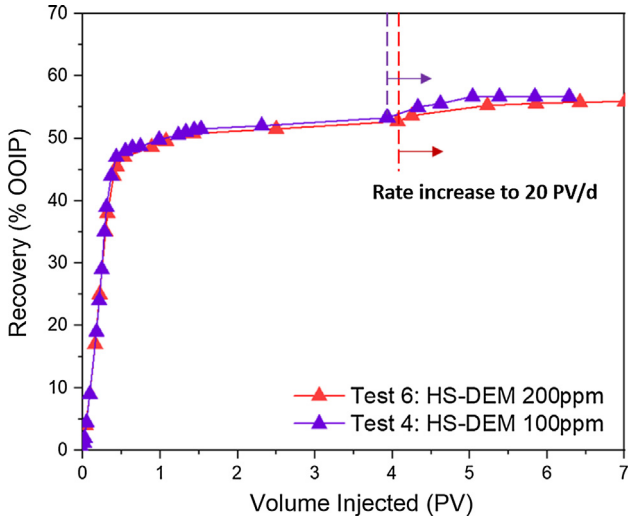

Fig. 16. Effect of DEM concentration on oil recovery at injection rate of 4 PV/d: Core #1.

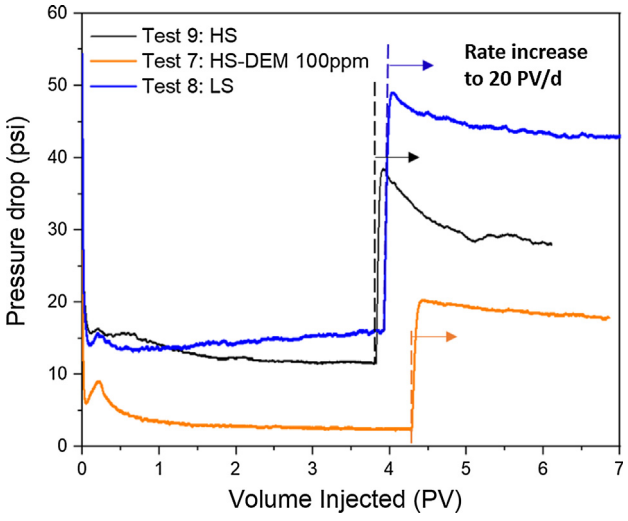

Fig. 18. Pressure drop profiles in the core without vugs with high salinity water (HS), low salinity water (LS), and high salinity water with 100 ppm of DEM (HS-DEM 100 ppm). The initial injection rate is 4 PV/d: Core #2.

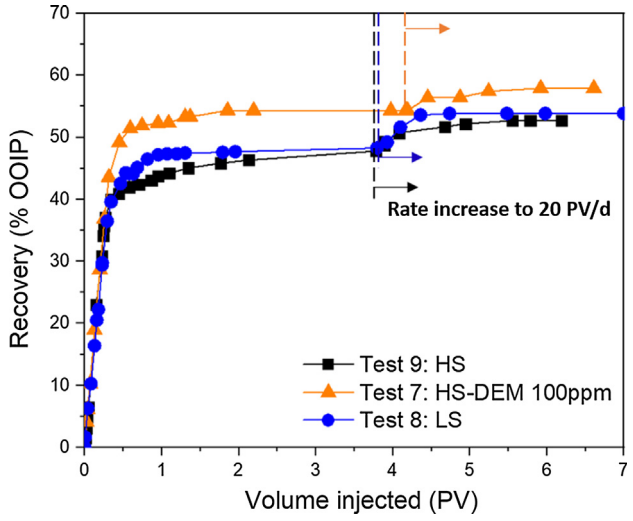

Fig. 17. Oil recovery performance at high salinity water (HS), low salinity water (LS), and high salinity water with 100 ppm of DEM: Initial injection rate is 4 PV/d): Core #2.

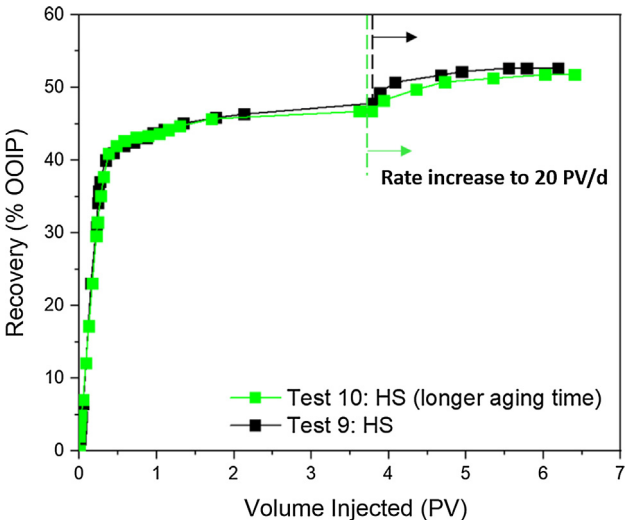

Fig. 19. Effect of longer aging time on oil recovery of waterflooding performance at injection rate of 4 PV/d: Core #2.

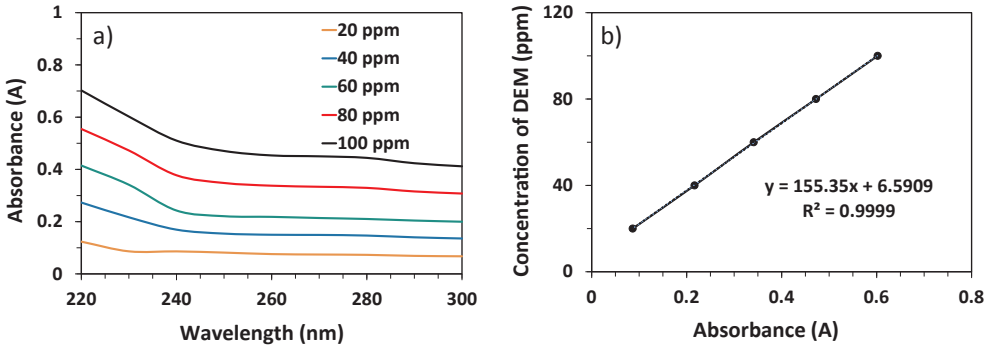

Fig. 20. (a) Absorbance spectra of demulsifier in high salinity brine, and (b) Calibration plot of demulsifier in high salinity brine.

Table 6
Adsorption at different concentrations of DEM in high salinity brine onto carbonate rock.

DEM concentration in brine (ppm)	Adsorption of DEM in rock (mg/g)	Equivalent Adsorption of DEM (mg/m^2)
20	0.4	5.8E−08
40	1.1	1.5E−07
60	1.6	2.3E−07
80	1.8	2.5E−07
100	2.0	2.8E−07

increased to 85 ppm at 5 PV of brine injection. There was no change in permeability to 10 PV. We have repeated the same test to higher PV injection. Results show no measurable effect of adsorption on permeability; the concentration of DEM in the injected brine and produced brine are the same after 14 PV injection [18]. All of our measurements indicate no significant adsorption in the carbonate core.

3.10. CMC measurement

Fig. 21 shows the surface tension of high salinity brine vs. the concentration of DEM. Based on the change in the slopes of the plots, two trendlines are obtained; the intersection of these two lines is at 30 ppm, which is the CMC. Based on CMC consideration, the injected concentration should be above 30 ppm. Based on emulsion testing a 100 ppm concentration may be selected. This will also allow for the low adsorption of the chemical. The upper limit is 200 ppm. The DEM is observed to be completely homogenized in the aqueous phase in the range of 200 ppm for a period of 7 days. In our coreflooding experiments, DEM in the range of 200 ppm was found to be in a single phase with the aqueous medium. The maximum concentration of the surfactant in aqueous phase for homogeneous solution is expected to deviate slightly by the salinity of the aqueous phase.

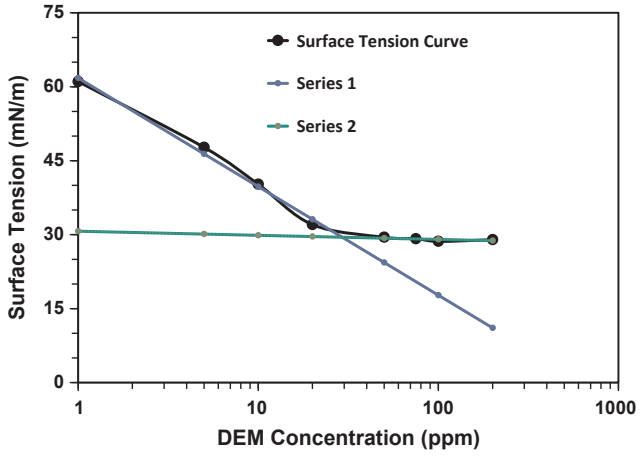

Fig. 21. Surface tension with respect to logarithmic scale of DEM concentration in high salinity brine; trendlines plotted for the two sections, Series 1 (1–20 ppm) and Series 2 (50–200 ppm), intersecting at CMC = 30 ppm.

4. Further discussions and conclusions

In conventional improved oil recovery, surfactants decrease the interfacial tension by orders of magnitude at a concentration which might be two order of magnitude higher than the surfactant used in this work. In the process from an increase in oil-water interfacial elasticity ($G' > G''$), the concentration at 100 ppm may be effective.

Our work has been conducted using dead oil, NaCl salt in the injected water, and room temperature. We used NaCl in the injected water to obtain consistent results without change of salt composition. Our ongoing measurements, based on a mixture of salts instead of NaCl shows a more pronounced interface elasticity effect. The effect of temperature can be expected to increase water-wetting and therefore may help the process by the DEM molecule compared to low salinity water injection. The use of a live oil in coreflooding, and development of the setup for high pressure interfacial viscoelasticity measurements are future steps. Recently we have conducted coreflooding at reservoir temperature and the effectiveness at high temperature is also observed.

The length of the two cores we have used varies from 2.2 to 2.5 in.. The permeability is high for a carbonate rock (about 40 md for Core #2 and about 450 md for Core #1) and porosity is also high (about 24% and 18% in Cores #1 and #2, respectively). We have used two different injection rates. The trend in recovery is about the same at both rates. The recovery results demonstrate the efficiency of the process from use of the DEM and the effect of interface elasticity increase. In Kar et al. [18] long carbonate cores (permeability of around 12 md) were used as mentioned in the introduction. The recovery trends are the same as in shorter cores (with high permeability) in this study.

The key conclusions drawn from this investigation are:

- The demulsifier used in this work has a very low adsorption to the carbonate rock, around 2 mg/g at 100 ppm concentration. The low adsorption is an important feature of the chemical.
- The CMC of the demulsifier molecule in the high salinity brine is about 30 ppm. The concentration of 100 ppm was selected for most of our measurements based on low adsorption and the CMC of 30 ppm.
- There is a mild increase in oil recovery from low salinity water injection compared to the high salinity water injection. High salinity water injection at 100 ppm of the demulsifier molecule has higher oil recovery than low salinity water injection.
- Two carbonate rocks (with and without vugs and with very different pore sizes) have similar trend in oil recovery and pressure drop profiles.
- The high oil recovery from injection of high salinity water with the

dissolved 100 ppm demulsifier molecule correlates with a significant increase in oil-water interface elasticity (reduction in phase angle). There is slightly higher oil recovery from low salinity injection compared to high salinity injection, which correlates with a mild increase in interface elasticity at low salt concentration.

- The demulsifier molecule used in this work at 100 ppm, not only increases interfacial elasticity but also mildly increases water-wetting. The wettability change is not significant due to very low adsorption at the fluid-rock surface. Most of the DEM molecules adsorb at the fluid-fluid interface increasing the interface elasticity, as shown by a decrease in phase angle. In general the process of low salinity and DEM addition to the injected brine at ultra-low concentration may be affected by multiple mechanisms. Based on interfacial rheology and coreflooding, we propose interface phase angle as a measure of elasticity.

5. SI conversion factor

1 psi = 6895 Pa
1 ppm = 1 mg/L
1 mD = m^2
atm = 101325 Pa
torr = 133.3224 Pa

CRediT authorship contribution statement

Hyeyoung Cho: Data acquisition, Original Draft, Writing. **Taniya Kar:** Investigation. **Abbas Firoozabadi:** Supervision.

Declaration of Competing Interest

The authors declare that they have no known competing financial interests or personal relationships that could have appeared to influence the work reported in this paper.

Acknowledgement

This work was supported by member companies of the Reservoir Engineering Research Institute (RERI). We appreciate the support.

Appendix A. Supplementary data

Supplementary data to this article can be found online at https://doi.org/10.1016/j.fuel.2020.117504.

References

[1] Aghaeifar Z, Strand S, Austad T, et al. Influence of formation water salinity/composition on the low-salinity enhanced oil recovery effect in high-temperature sandstone reservoirs. Energy Fuels 2015;29(8):4747–54. https://doi.org/10.1021/acs.energyfuels.5b01621.
[2] Aslan S, Najafabadi NF, Firoozabadi A. Non-monotonicity of the Contact Angle from NaCl and $MgCl_2$ concentrations in two petroleum fluids on atomistically smooth surfaces. Energy Fuels 2016;30(4):2858–64. https://doi.org/10.1021/acs.energyfuels.6b00175.
[3] Acevedo S, Escobar G, Gutiérrez LB, Rivas H, Gutiérrez X. Interfacial rheological studies of extra-heavy crude oils and asphaltenes: role of the dispersion effect of resins in the adsorption of asphaltenes at the interface of water-in-crude oil emulsions. Colloids Surf, A 1993;71:65–71. https://doi.org/10.1016/0927-7757(93)80028-D.
[4] Bartels W-B, Mahani H, Berg S, Hassanizadeh SM. Literature review of low salinity waterflooding from a length and time scale perspective. Fuel 2019;236:338–53. https://doi.org/10.1016/j.fuel.2018.09.018.
[5] Bernard GG. Effect of floodwater salinity on recovery of oil from cores containing clays. In: Presented at the SPE California Regional Meeting, Los Angeles, California, 26-27 October. SPE-1725-MS; 1967. DOI: 10.2118/1725-MS.
[6] Bidhendi MM, Garcia-Olvera G, Morin B, et al. Interfacial viscoelasticity of crude oil/brine: an alternative enhanced-oil-recovery mechanism in smart waterflooding. SPE J. 2018;23(3):803–18. https://doi.org/10.2118/169127-PA. SPE-169127-PA.
[7] Chávez-Miyauchi TE, Firoozabadi A, Fuller GG. Nonmonotonic elasticity of the crude oil-brine interface in relation to improved oil recovery. Langmuir 2016;32(9):2192–8. https://doi.org/10.1021/acs.langmuir.5b04354.
[8] Chávez-Miyauchi TE, Lu Y, Firoozabadi A. Low Salinity Water Injection in Berea Sandstone: Effect of Wettability, Interface Elasticity, and Acid and Base Functionalities. Fuel, In press. DOI: 10.1016/j.fuel.2019.116572.
[9] Emadi A, Sohrabi M. Visual Investigation of Oil Recovery by Low Salinity Water Injection: Formation of Water Micro-Dispersions and Wettability Alteration. In: Presented at the SPE Annual Technical Conference and Exhibition, New Orleans, Louisiana, 30 September-2 October. SPE-166435-MS; 2013.
[10] Fan Y, Simon S, Sjöblom J. Interfacial Shear Rheology of Asphaltenes at Oil–Water Interface and its Relation to Emulsion Stability: Influence of Concentration, Solvent Aromaticity and Nonionic Surfactant. Colloids and Surfaces A: Physicochemical and Engineering Aspects 366(1-3): 120–128, 2010. https://www.sciencedirect.com/science/article/abs/pii/S0927775710003316.
[11] Freer EM, Svitova T, Radke CJ. The role of interfacial rheology in reservoir mixed wettability. J Petrol Sci Eng 2003;39(1-2):137–58https://www.sciencedirect.com/science/article/abs/pii/S0920410503000457.
[12] Hamouda AA, Valderhaug OM. Investigating enhanced oil recovery from sandstone by low-salinity water and fluid/rock interaction. Energy Fuels 2014;28(2):898–908. https://doi.org/10.1021/ef4020857.
[13] Ilyin S, Arinina M, Polyakova M, Bondarenko G, Konstantinov I, Kulichikhin V, et al. Asphaltenes in heavy crude oil: designation, precipitation, solutions, and effects on viscosity. J. Petrol. Sci. Eng. 2016;147:211–7. https://doi.org/10.1016/j.petrol.2016.06.020.
[14] Jadhunandan P. Effects of brine composition, crude oil and aging conditions on wettability and oil recovery. PhD dissertation, New Mexico Institute of Mining and Technology, Socorro, New Mexico (October 1991), 1990.
[15] Jadhunandan P, Morrow NR. Spontaneous imbibition of water by crude oil/brine/rock systems. Situ 1991;15(4):319–45.
[16] Kamal MS, Hussein IA, Sultan AS. Review on surfactant flooding: phase behavior, retention, IFT, and field applications. Energy Fuels 2017;31(8):7701–20. https://doi.org/10.1021/acs.energyfuels.7b00353.
[17] Kang W, Yin X, Yang H, Zhao Y, Huang Z, Hou X, et al. Demulsification performance, behavior and mechanism of different demulsifiers on the light crude oil emulsions. Colloids Surf A: Physicochem Eng Aspects 2018;545:197–204. https://doi.org/10.1016/j.colsurfa.2018.02.055.
[18] Kar T, Chávez-Miyauchi TE, Firoozabadi A, Pal M. A new process for improved oil recovery from water injection by a functional molecule at 100 ppm concentration. Presented at the SPE Annual Technical Conference and Exhibition, Calgary, Alberta, Canada, 30 September – 2 October. SPE-196036-MS 2019. https://doi.org/10.2118/196036-MS.
[19] Kazempour M, Kiani M, Nguyen D, et al. Boosting oil recovery in unconventional resources utilizing wettability altering agents: successful translation from laboratory to field. Presented at the SPE improved oil recovery conference, Tulsa, Oklahoma, 14-18 April. SPE-190172-MS 2018. https://doi.org/10.2118/190172-MS.
[20] Li Y. Oil recovery by low salinity water injection into a reservoir: a new study of tertiary oil recovery mechanism. Transp Porous Med 2011;90(2):333–62. https://doi.org/10.1007/s11242-011-9788-8.
[21] Lin CL, Miller JD. Pore structure and network analysis of filter cake. Chem Eng J 2000;80(1–3):221–31. https://doi.org/10.1016/S1383-5866(00)00094-0.
[22] Mandal A, Samanta A, Bera A, et al. Characterization of oil-water emulsion and its use in enhanced oil recovery. Ind Eng Chem Res 2010;49(24):12756–61. https://doi.org/10.1021/ie101589x.
[23] Marsden SS. Wettability-Its measurement and application to waterflooding. J Jpn Assn Pet Tech 1965;30(1):1–10.
[24] Martin JC. The effects of clay on the displacement of heavy oil by water, Presented at the Venezuelan Annual Meeting, Caracas, Venezuela, 14-16 October. SPE-1411-G; 1959. DOI: 10.2118/1411-G.
[25] Morrow N, Buckley J. Improved oil recovery by low-salinity waterflooding. J Petrol Technol 2011;63(5):106–12. https://doi.org/10.2118/129421-JPT. SPE-129421-JPT.
[26] Negin C, Ali S, Xie Q. Most common surfactants employed in chemical enhanced oil recovery. Petroleum 2017;3(2):197–211https://www.sciencedirect.com/science/article/pii/S2405656116300621.
[27] Owens WW, Archer DL. The effect of rock wettability on oil-water relative permeability relationships. J Petrol Technol 1971;23(7):873–8. https://doi.org/10.2118/3034-PA. SPE-3043-PA.
[28] Pradilla D, Simon S, Sjöblom J. Mixed interfaces of asphaltenes and model demulsifiers, part II: study of desorption mechanisms at liquid/liquid interfaces. Energy Fuels 2015;29(9):5507–18. https://doi.org/10.1021/acs.energyfuels.5b01302.
[29] Pradilla D, Simon S, Sjöblom J, Samaniuk J, Skrzypiec M, Vermant J. Sorption and interfacial rheology study of model asphaltene compounds. Langmuir 2016;32:2900–11. https://doi.org/10.1021/acs.langmuir.6b00195.
[30] Rezaei N, Firoozabadi A. Macro- and microscale waterflooding performances of crudes which form w/o emulsions upon mixing with brines. Energy Fuels 2014;28(3):2092–103. https://doi.org/10.1021/ef402223d.
[31] Sagi AR, Tomas CP, Brian Y et al. Laboratory Studies for Surfactant Flood in Low-Temperature, Low-Salinity Fractured Carbonate Reservoir. In: Presented at the SPE International Symposium on Oilfield Chemistry, The Woodlands, Texas, 8-10 April. SPE 164062-MS; 2013. DOI: 10.2118/164062-MS.
[32] Sheng JJ. Critical review of low-salinity waterflooding. J Petro Sci Eng 2014;120:216–24. https://doi.org/10.1016/j.petrol.2014.05.026.
[33] Spiecker PM, Kilpatrick PK. Interfacial rheology of petroleum asphaltenes at the oil− water interface. Langmuir 2004;20(10):4022–32. https://doi.org/10.1021/la0356351.

[34] Stalder AF, Kulik G, Sage D, et al. A snack-based approach to axcurate determination of both contact points and contact angles. Colloids Surf A Physicochem Eng Asp 2006;286(1–3):92–103. https://doi.org/10.1016/j.colsurfa.2006.03.008.
[35] Stalder AF, Melchior T, Müller M, et al. Low-bond axisymmetric drop shape analysis for surface tension and contact angle measurements of sessile drops. Colloids Surf A Physicochem Eng Asp 2010;364(1–3):72–81. https://doi.org/10.1016/j.colsurfa.2010.04.040.
[36] Sun M, Mogensen K, Bennetzen M, et al. Demulsifier in injected water for improved recovery of crudes that form water/oil emulsions. SPE Res Eval Eng 2016;19(4):1–9. https://doi.org/10.2118/180914-PA. SPE-180914-PA.
[37] Sztukowski DM, Yarranton HW. Rheology of asphaltene-toluene/water interfaces. Langmuir 2005;21:11651–8. https://doi.org/10.1021/la051921w.
[38] Tang G, Firoozabadi A. Effect of pressure gradient and initial water saturation on water injection in water-wet and mixed-wet fractured porous media. SPE Res Eval Eng 2001;4(6):516–24. https://doi.org/10.2118/74711-PA. SPE-74711-PA.
[39] Tang GQ, Morrow NR. Salinity, temperature, oil composition, and oil recovery by waterflooding. SPE Reserv Eng 1997;12(4):269–76. https://doi.org/10.2118/36680-PA. SPE-36680-PA.
[40] Tang GQ, Morrow NR. Influence of brine composition and fines migration on crude oil/brine/rock interactions and oil recovery. J Petrol Sci Eng 1999;24(2–4):99–111. https://doi.org/10.1016/S0920-4105(99)00034-0.
[41] Torrijos IDP, Puntervold T, Strand S, et al. Experimental study of the response time of the low-salinity enhanced oil recovery effect during secondary and tertiary low-salinity waterflooding. Energy Fuels 2016;30(6):4733–9. https://doi.org/10.1021/acs.energyfuels.6b00641.
[42] Varadaraj R, Brons C. Molecular origins of crude oil interfacial activity. Part 4: oil-water interface elasticity and crude oil asphaltene films. Energy Fuels 2012;26(12):7164–9. https://doi.org/10.1021/ef300830f.
[43] Wang Y, Lin CL, Miller JD. Improved 3D image segmentation for X-ray tomographic analysis of packed particle beds. Miner Eng 2015;83:185–91. https://doi.org/10.1016/j.mineng.2015.09.007.
[44] Yassin MR, Ayatollahi S, Rostami B, et al. Micro-emulsion phase behavior of a cationic surfactant at intermediate interfacial tension in sandstone and carbonate rocks. J Energy Resour Asme 2015;137(1). https://doi.org/10.1115/1.4029267. 12905-1-12905-12.